Computational and Structural Biotechnology Journal 23 (2024) 771–782

Contents lists available at ScienceDirect

Computational and Structural Biotechnology Journal

journal homepage: www.elsevier.com/locate/csbj

Effects of age on differential resistance to duck hepatitis A virus genotype 3 in Pekin ducks by 16 S and transcriptomics

Suyun Liang [a], Meixi Lu [a], Daxin Yu [a], Guangnan Xing [a], Zhanqing Ji [a], Zhanbao Guo [a], Qi Zhang [a], Wei Huang [a], Ming Xie [a], Shuisheng Hou [a,*]

[a] Institute of Animal Sciences, Chinese Academy of Agricultural Sciences, Beijing 100193, China

ARTICLE INFO

Keywords:
Pekin duck
Intestinal microbiota
Age
DHAV-3
Resistance differences

ABSTRACT

Duck hepatitis A virus genotype 3 (DHAV-3) is the major cause of viral hepatitis in ducks in Asia. Previous studies have shown that ducklings younger than 21 days are more susceptible to DHAV-3. To elucidate the mechanism by which age affects the differential susceptibility of Pekin ducks to DHAV-3, intestinal ($n = 520$), liver ($n = 40$) and blood ($n = 260$) samples were collected from control and DHAV-3-infected ducks at 7, 10, 14, and 21 days of age. Comparisons of plasma markers, mortality rates, and intestinal histopathological data showed that the resistance of Pekin ducks to DHAV-3 varied with age. 16 S sequencing revealed that the ileal microbial composition was influenced by age, and this correlation was greater than that recorded for caecal microbes. *Candidatus Arthromitus*, *Bacteroides*, *Corynebacterium*, *Enterococcus*, *Romboutsia*, and *Streptococcus* were the differntially abundant microbes in the ileum at the genus level after DHAV-3 infection and were significantly correlated with 7 differentially expressed genes (DEGs) in 7- and 21-day-old ducklings. 3 immunity-related pathways were significantly different between 7- and 21-day-old ducklings, especially for *IFIH1*-mediated induction of the interferon-alpha/beta pathway, which induces differential production of CD8(+) T cells and was influenced by a combination of differentially abundant microbiota and DEGs. We found that microbes in the ileum changed regularly with age. The intestinal microbiota was associated with the expression of genes in the liver through IFIH1-mediated induction of the interferon-alpha/beta pathway, which may partially explain why younger ducklings were more susceptible to DHAV-3 infection.

1. Introduction

The poultry industry is the focus of livestock farming development because of its favourable meat-to-feed ratio and short production cycle. Globally, meat consumption has shifted towards poultry meat, with almost all countries increasing their consumption of poultry meat [1,2]. Pekin ducks constitute a major part of the global poultry industry. These ducks exhibit a high growth rate, good feed conversion, a high lean meat percentage, a low skin/fat ratio, and a high dressing percentage and have become the most widely reared ducks in the duck industry [3]. More than 200 million ducks are slaughtered for their meat in the United States and the European Union each year [4,5]. Although the Pekin duck industry is large, few studies have investigated the effects of the composition and structure of the intestinal flora on the growth, development, and health of Pekin ducks [6,7]. The intestinal flora influences the ability of host animals to digest and absorb nutrients [8], the immune response [9], the synthesis of amino acids and vitamins [10], and the proliferation of pathogenic microbes [11]. Therefore, the study of the composition and structure of the intestinal flora of ducks is essential for the healthy development of the duck industry.

The rate of infection for susceptible individuals varies significantly with age [12], and younger individuals are more susceptible to infection, playing a strong role in the transmission of pathogens [13]. One reason for this finding is that younger individuals have an inadequate immune response, resulting in a lower resistance to infection than in adults [14]. Some studies have reported a general pattern, suggesting that infection rates increase in early childhood years and then decrease with age [15]. Similar results have also been reported in livestock diseases; for example, young sheep have significantly lower proportions of CD4(+) and CD8(+) lymphocytes. In addition, their blood lymphocytes produce less interferon-7 in culture and have a weaker antibody response than those of mature animals [16]. In the Pekin duck industry,

* Correspondence to: Institute of Animal Sciences, Chinese Academy of Agricultural Sciences, No. 2 Yuanmingyuan West Road, Haidian, Beijing 100193, China. *E-mail address:* houss@263.net (S. Hou).

https://doi.org/10.1016/j.csbj.2024.01.005
Received 24 September 2023; Received in revised form 9 January 2024; Accepted 14 January 2024
Available online 17 January 2024

duck viral hepatitis (DVH) is a highly contagious, fatal disease of young ducklings, and ducklings less than three weeks old are highly susceptible to this disease [17]. DVH can cause up to 95% mortality in ducklings less than one week old [18]. Age of Pekin ducklings strongly influences the differences in susceptibility to DVH. In another study, we showed that high genomic copy numbers of DHAV-3, which is the most prevalent pathogen causing DVH in the Asian duck industry [19,20], occurred in the intestinal tissues of susceptible ducklings. Additionally, the viral load in the intestinal tissues of resistant ducks was significantly lower than that in the intestinal tissues of susceptible ducks [21], suggesting that the intestinal load is associated with the susceptibility of Pekin ducks to DHAV-3. None of these studies investigated the changes induced in the intestinal microbiota of Pekin ducks following viral infection, although the microbiota is known to be the primary mediator and regulator of innate and adaptive immune functions.

We conducted this study to understand the influence of host–microbe interactions on different susceptibilities from the perspective of the "gut-liver axis". In this study, the composition and structure of the intestinal microbiota of Pekin ducks on different days were determined, as well as the changes in intestinal microbes that occurred after viral infection and the relationship between the intestinal microbiota and disease resistance. To conduct this study, we designed three experiments. We assessed the intestinal microbiota of 7-day-old, 10-day-old, 14-day-old, and 21-day-old Pekin ducks, all of which had the same genetic background. We analysed the intestines of ducklings of different age groups after DHAV-3 infection to determine the effect of the virus on intestinal microbes, using the uninfected group as a control. Finally, transcriptomic analysis was performed to identify differentially expressed genes (DEGs) for different age groups, and the results were combined with an analysis of differentially abundant microbes to determine the influence of these microbes on the disease resistance in Pekin ducks.

2. Materials and methods

2.1. Ethics statement

Animal experiments were performed following the guidance and under the approval of the Animal Welfare and Ethics Committee of China Agricultural University and the animal care and use committee of the Institute of Animal Sciences of the Chinese Academy of Agricultural Sciences (IAS2022–116).

2.2. Virus

DHAV-3 112803 was originally isolated from a dead duckling during an outbreak of DVH in China in 2011 [22]. The virus was propagated in 9-day-old embryonating Pekin duck eggs and stored at − 80 °C. Using 10-day-old duck embryos, the titre of DHAV-3 was determined to be $10^{6.25}$ 50% egg lethal dose (ELD_{50})/0.1 mL.

2.3. Animal experimental design

The Z2 strain of Pekin ducks was used in this study. When the ducks reached approximately 30 weeks of age, 10 males and 40 females were collected to construct families. The females were fed separately, each male was mated with only four fixed females, and the ducks were reared separately and fed a grower diet (air-dried basis, 12.6 MJ/kg ME and 17.6 g/kg CP). When the ducks reached 40 weeks of age, eggs were collected in four batches and marked according to the pedigree. All ducks were raised with common diets, and all nutrients met the recommendations for ducks established in the Nutrient Requirements of Meat-type Ducks of China [23]. Feed and water were provided ad libitum during the experiment.

For DHAV-3 challenge, ducklings from the 7-day group (n = 100), 10-day group (n = 100), 14-day group (n = 100) and 21-day group (n = 100) from the same families were selected and named In7, In10, In14 and In21, respectively, and these ducklings were infected on the same day by intramuscular injection. As a control, ducklings from the 7-day (n = 15), 10-day (n = 15), 14-day (n = 15) and 21-day (n = 15) groups from the same families were selected and named C7, C10, C14 and C21, respectively, and these ducklings were inoculated with PBS. The mortality was observed every 6 h during the 12–72 h post inoculation (hpi).

2.4. Tissues collection

Two hundred ducklings from the challenge group and 60 ducklings from the control group were selected, and samples were taken at 18 hpi. The remaining ducks were used to observe mortality, and the mortality rates of each group were recorded in detail. A total of 260 ileum, 260 caecum, and 260 blood samples were collected, and five duck livers from C7, C10, C14, C21, In7, In10, In14 and In21 were collected. Ileum and caecum mucosa samples were stored at − 80 °C and subjected to 16 S sequencing; blood samples were subjected to plasma biochemical assays; and liver tissues were subjected to RNA-seq. Three ducks were randomly selected from each group for tissue collection. A total of 24 samples were included, including 12 ileum tissues and 12 caecum tissues. These tissues were subjected to haematoxylin-eosin (H&E) staining analysis. The number of DHAV-3 copies in the ileum was determined as described previously [20].

2.5. DNA extraction, 16 S rRNA sequencing and library preparation of ileum and caecum

A total of 520 intestinal samples (260 ileum mucosa and 260 caecum mucosa samples) were collected, and 0.2 g of each sample was added to a PowerBead tube. Extraction was performed using the MagPure Stool DNA LQ Kit (Magen, Guangzhou, China) following the manufacturer's instructions. The DNA was checked for purity on a Nanodrop (Thermo Scientific, USA), and DNA concentrations were measured using a Qubit 2.0 fluorometer (Thermo Fisher Scientific, MA, USA). The DNA was stored at − 80 °C until sequencing.

The V3-V4 region of the 16 S rRNA gene was amplified using the primers 341 F/805 R. The PCR program was performed under the following conditions: denaturation for 3 min at 95 °C; 25 cycles of denaturation at 95 °C for 30 s, 55 °C for 30 s, and 72 °C for 15 s; and a final extension at 72 °C for 5 min. The purified DNA samples were subsequently quantified using a Qubit 2.0 fluorometer, sequencing libraries were constructed using the NEBNext® Ultra™ II DNA Library Prep Kit for Illumina (New England Biolabs, MA, USA) following the manufacturer's instructions, and index codes were added. The library quality was assessed using a Qubit 2.0 fluorometer. Finally, the library was sequenced on an Illumina NovaSeq 6000 platform at Wuhan Benagen Technology Company Limited (Wuhan, China).

2.6. 16 S rRNA gene data processing and bioinformatic analysis

Cutadapt (v.3.5) software [24] was used to identify and remove primer sequences, and length filtering was performed to obtain clean sequences. For the identification of feature sequences (amplicon sequence variants, ASVs), DADA2 [25] was used to filter the raw data, splice paired-end reads and remove chimeric sequences. Then, QIIME2 software [26] was used to filter the low-abundance ASVs, and all samples were flattened with the minimum number of sequences. Subsequently, the bacterial ASVs were assigned to taxonomic groups using the SILVA database (https://www.arb-silva.de/) for species annotation.

The alpha diversity indices, including the Shannon, Simpson, Chao1 and ACE indices, were calculated using QIIME2 software. The beta diversity was calculated using the R package to investigate the community dissimilarities among the treatments. In addition, analysis of similarities (ANOSIM) was conducted to examine the significance of the differences between groups and the significance of the differences in distance

between and within groups. Statistical significance was determined through one-way analysis of variance (ANOVA) followed by post hoc Tukey's test. Functional inference was made from the Kyoto Encyclopedia of Genes and Genomes (KEGG) pathway and Clusters of Orthologous Groups of proteins (COG) databases.

2.7. Liver RNA extraction and transcriptome sequencing

Forty liver tissues were used; 15 mg of each liver sample was weighed, ground in liquid nitrogen and extracted using a Total RNA Kit I (Omega: No. R6834–02). Libraries were constructed using the MGIEasy RNA Library Prep Kit for BGI® and sequenced by combining probe anchored polymerization (cPAS) technology (DNBSEQ, BGI) with an average sequencing depth of approximately 6 × .

2.8. Analyses of RNA-seq data

To ensure the reliability of the information analysed, the raw sequencing data were filtered to remove low-quality and contaminated reads, thus obtaining clean reads. Quality control of the filtered data was performed using fastQC (v0.11.9) [27]. The filtered sequences were aligned with the reference genome (GenBank assembly accession: GCA_015476345.1) using STAR (v2.7.9a) [28]. The number of reads per sample compared to that of each transcript was obtained using RSEM [29] and converted to fragments per kilobase per million bases (FPKM) values. DEGs were screened using DESeq2 (v1.26.0) [30] with screening thresholds of a false discovery rate (FDR) < 0.05 and $|\log_2\text{FoldChange}| > 1$.

2.9. Enzyme-linked immunosorbent assay (ELISA)

Blood samples were collected in anticoagulant-free tubes and centrifuged at 3000 × *g* for 15 min to obtain the serum. Standard wells, blank wells and sample wells were set up. Fifty microlitres of each of the standards at different concentrations was added to the standard wells. Colorants A and B and termination solution were added to the blank wells for zeroing. Fifty microlitres of sample and 50 μl of antigen working solution were added to each sample well. After gently shaking and mixing, the plates were covered with sealing film and incubated at 37 °C for 30 min. The sealing film was removed, the liquid was discarded, the plates were shaken dry, and each well was filled with washing solution and allowed to rest for 30 s before the solution was discarded. This process was repeated 5 times, after which the wells were patted dry. HRP-conjugate reagent (100 μl) was added to each well, and the mixture was allowed to react at 37 °C for 30 min. The plates were washed 5 times again and patted dry. Chromogen Solution A (50 μl) and Chromogen Solution B (50 μl) were added to each well, and the plate was incubated in the dark for 15 min at 37 °C. Then, 50 μl of Stop Solution was added to each well to terminate the reaction. The optical density of each well was measured sequentially at 450 nm using a blank well as the zero value. The regression equation for the standard curve was calculated using ELISAcalc based on the concentration and OD values, and the logistic curve was chosen as the fitting model. Immunoglobulin A (IgA), interferon alpha (IFN-α) and C-reactive protein (CRP) levels were determined by ELISA. The ranges of IgA, IFN-α and CRP were 0–6.1 g/L, 0–125 pg/mL and 0–500 pg/mL, respectively. The R^2 values of the standard curves were 0.99998, 0.99993 and 0.99997. The sensitivity of the kit was < 7 in each batch, and the recovery rate was approximately 103%.

2.10. H&E staining and villus height (VH) measurement

The ileum tissues were fixed in 4% buffered formaldehyde solution (pH 7.4) for 24 h. Following dehydration, the tissues were embedded in paraffin and cut into 5-μm-thick sections. Sections were stained with haematoxylin and eosin and observed under a light microscope (Olympus, Japan). Observations were made under an optical microscope (SONY, Alpha6000), and Image-Pro Plus 6.0 software was used to measure the VH at 100 × .

2.11. Flow cytometry

The flow cytometry procedure was performed as previously described [31]. The antibody used for the CD8(+) T-cell assay was APC/Cyanine7-conjugated anti-human CD8 (No. 344714; Biolegend). Blood samples treated with anticoagulant agents were taken from 3 individuals in each group.

2.12. Distance correlations between DEGs and differentially abundant microbes

We used Euclidean distances for transcriptomic data and Bray distances for phenotypic data. Mantel tests were performed between DEGs and differentially abundant microbes. The "linkET" [32], "ggtext", "dplyr" and "ggplot2" R (v4.2.2) software packages (http://github.com) were used in these analyses.

2.13. Data analysis

Phenotypic data are expressed as the mean ± standard deviation (SD). Differences between two groups were compared using Student's *t* test in GraphPad Prism 6.0 (GraphPad Software, Inc., San Diego, CA, USA). The Kruskal—Wallis test was used for multiple-group comparisons. $P < 0.05$ was considered to indicate statistical significance.

3. Results

3.1. Intestinal development and blood immunity indices in Pekin ducks at different ages

VH was measured in the ileum and caecum of C7, C10, C14, and C21. As shown in Fig. 1A, the VH in the caecal tissues fluctuated but increased overall with age, with the VH at 14 days being significantly greater than that at 7, 10 and 21 days. In the ileum, the VH increased with age and was significantly greater at 21 days than at 7, 10 and 14 days.

The concentrations of IgA, IFN-α and CRP were measured in the different control groups. As shown in Fig. 1B, IgA showed an increasing trend, and its concentration in C21 was significantly higher than that in the other three groups ($P < 0.05$). There was no significant difference in the IgA concentration among the three groups (C7, C10 and C14). IFN-α followed the same trend as IgA, but only the C7 group had significantly lower concentrations of IFN-α than the C10, C14 and C21 groups. The concentration of CRP decreased and then increased with age, but the difference was not significant.

3.2. Sequencing result summary

In total, 520 samples were sequenced, and 55,625,518 paired reads were obtained after Illumina sequencing (Additional file 1: Table S1). Rarefaction curves generated from the amplicon sequence variants (ASVs) suggested that high sampling coverage was achieved in all samples, suggesting that the sequencing depth was sufficient for the investigation of the intestinal microbiota (Additional file 2: Fig. S1). The number of ASVs (including those in the control and challenge groups) at 7 days of age was lower than that in the other three age groups, and the number of cooccurring ASVs increased with age, as expected (Additional file 2: Fig. S2).

3.3. Ileal microbial diversity and composition showed age-related changes

The richness (Chao1 and ACE) and diversity (Shannon and Simpson) indices of the ileum increased with age, although there were no

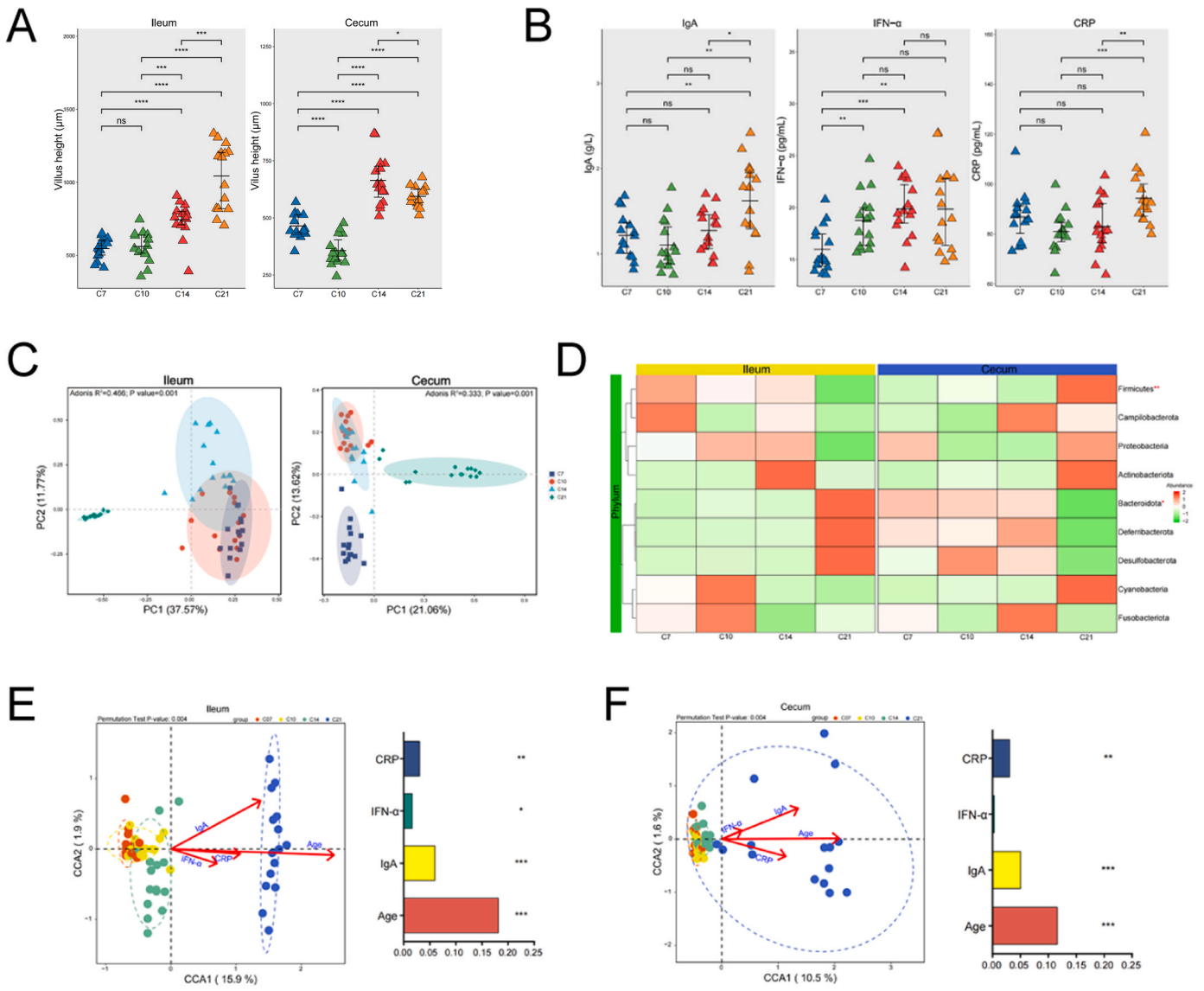

Fig. 1. Age-related changes (in days) in the ileum and caecum. **A.** Villus height in ileal and caecal tissues of Pekin ducks at 7, 10, 14, and 21 days after hatching. **B.** Plasma levels of immunoglobulin A (IgA), interferon alpha (IFN-α) and C-reactive protein (CRP) in Pekin ducks at 7, 10, 14, and 21 days after hatching. **C.** Principal coordinate analysis (PCoA) of the microbial composition of the ileum and caecum based on the Bray—Curtis distance. **D.** Heatmap of microbes in the ileum and caecum at the phylum level. Canonical correlation analysis (CCA) of microbial and phenotypic indicators in the ileum (**E**) and caecum (**F**); * , $P < 0.05$; ** , $P < 0.01$; *** , $P < 0.001$.

significant differences between C10 and C14 ($P > 0.05$). However, there were no age-related changes in microbial diversity in the caecum (Additional file 2: Fig. S3).

Based on the Bray—Curtis distance, the scatter distances in the principal coordinate analysis (pCoA) plots of the ileal group showed that the samples within the C21 group were less different and clearly separated from the other three groups. C7, C10 and C14 showed a certain trend with age in days, with C7 being separable from C14 (Fig. 1C). Hierarchical clustering based on ASV information was also generated. Ileum samples from C7 and C10 were grouped tightly, followed by those from C14, and the ASVs from the four groups could be separated into two lineages. Similar results were also found via pCoA using weighted and unweighted UniFrac metrics (Additional file 2: Fig. S4). However, the results for the relationships of the four groups from the caecum differed among the multiple variants.

In the ileum, *Firmicutes* was the most abundant phylum, accounting for more than 60% of the total resident bacteria. *Firmicutes* was the most abundant phylum in the caecum of the C21 group, and *Bacteroidetes* was the most abundant phylum in C7, C10 and C10 (Additional file 2: Fig. S5). In the ileum, the abundance of *Firmicutes* decreased with age, and the opposite was true for *Bacteroidota*, *Desulfobacterota* and *Deferribacterota*. In the caecum, the abundance of *Firmicutes* and *Actinobacteria* increased with age, and that of *Bacteroidetes* decreased with age. The ileum and caecum showed significant differences in *Firmicutes* and *Bacteroidetes* abundances (Fig. 1D; Additional file 1: Table S2) (Kruskal—Wallis test, $P < 0.05$).

The canonical correlation analysis (CCA) results for microbial composition and plasma immunological indicators for different ages are shown in Figs. 1E and 1F. In C7, C10 and C14, the IgA, IFN-α and CRP levels were negatively correlated with age. Some of the microbial components of the ileum were shared among C7, C10 and C14, and the PERMANOVA test confirmed highly significant differences between these three groups and C21 ($P = 0.004$). The abundances of various taxa showed that microbial composition was much more strongly correlated with age than with other factors ($P < 0.001$, $r^2 = 0.1816$). However, most of the microbial composition of the caecum was shared among C7,

C10 and C14, and age was the most relevant factor ($P < 0.001$, $r^2 = 0.1162$).

3.4. Phenotypic changes in ducklings and ileal microbial composition after infection with DHAV-3

As shown in Fig. 2A, after infection with DHAV-3, the mortality rate of ducklings was 68% in the In7 group, 34% in the In10 group, 4% in the In14 group and 0% in the In21 group. The IgA concentrations were significantly higher in the In7 and In21 groups than in the control group. IFN-α levels were significantly higher in the In7 group than in the C7 group, but no significant differences were observed in the other three groups. CRP levels at 7 days of age were not influenced by DHAV-3 infection, but they were significantly different in the In10, In14 and In21 groups compared with those in the control group (Fig. 2B).

In the ileum, the number of DHAV-3 genome copies was greatest in the In7 subgroup, significantly greater than that in the In14 and In21 groups, but not significantly different from that in the In10 group (Fig. 2C). Pathological histological analysis revealed that the degree of damage to the intestine caused by DHAV-3 infection decreased with age (Fig. 2D), with severe haemorrhage and inflammatory cell infiltration observed in the intestinal tissues of 7-day-old ducklings and with the number of lesions decreasing with age.

The ileum showed more regular age-related changes in microbial composition than did the caecum. Therefore, the ileum was used to study changes in microbial composition following DHAV-3 infection. As shown in Fig. 3A, the number of ASVs per group increased more than 2-fold after infection, with the highest increase of 6-fold observed in the 7-day-old group. DHAV-3 infection significantly altered the composition of microbes in the ileum (Additional file 1: Table S3). The CCA results showed that age and viral infection were positively correlated with microbial diversity, and the amount of variance explained by their interaction was 1.1141 ($P < 0.001$; Fig. 3B). The results of the LEfSe analysis showed that the predominance of microbes decreased in each group after infection, but there were no significant changes in the four microbes at the genus level after infection (Fig. 3C; Additional file 1:

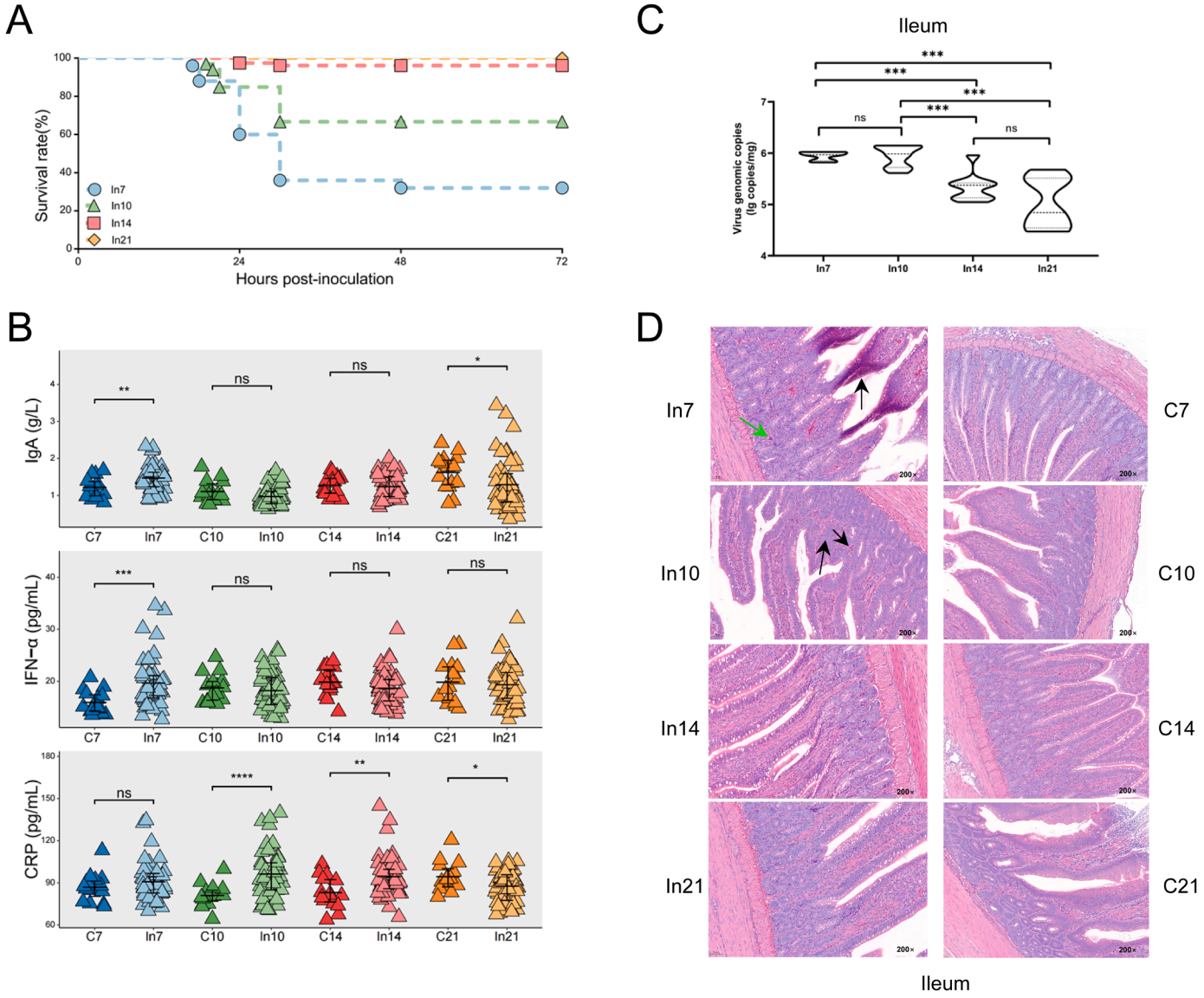

Fig. 2. Phenotypic changes after DHAV-3 infection. **A**. Mortality curves of ducklings infected with DHAV-3 at 7, 10, 14, and 21 days after hatching. **B**. Changes in plasma immunoglobulin A (IgA), interferon alpha (IFN-α) and C-reactive protein (CRP) levels after infection with DHAV-3 in ducklings at 7, 10, 14, and 21 days after hatching. **C**. Detection of viral load in challenge groups. The number of viral genomic copies was calculated as $\log_{10}$ virus RNA copies/mg. For each group, ileum tissues were sampled at 18 h p.i. ns, $P > 0.05$; *** , $P < 0.001$. **D**. Pathological histology of ileal tissue after DHAV-3 infection; 200 × . The black arrow indicates haemorrhage and congestion, the green arrow indicates focal lymphocytic aggregations.

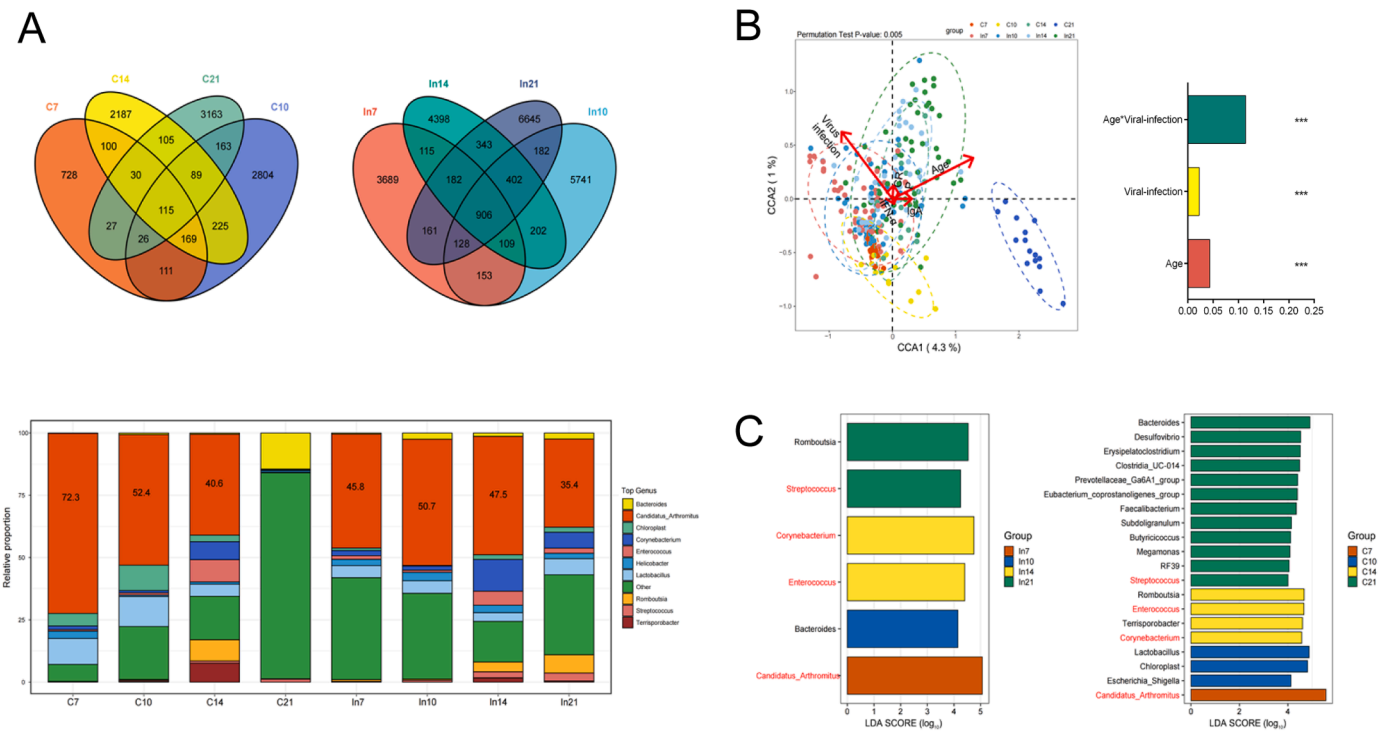

Fig. 3. Ileal microbial changes after DHAV-3 infection. **A**. Number of amplicon sequence variants (ASVs) in the ileum of ducklings before (left) and after (right) DHAV-3 infection at 7, 10, 14, and 21 days after hatching. **B**. Canonical correlation analysis (CCA) of microbial and phenotypic indicators in the ileum. *** , $P < 0.001$. **C**. LEfSe analysis in ileal microbial of Pekin ducks at 7, 10, 14, and 21 days after hatching. Microbes marked in red were present before and after infection with DHAV-3.

Table S4).

3.5. Significantly differences were found in 3 immunity-related pathways

The results of the Gene Ontology (GO) enrichment analysis of the DEGs revealed that 16 GO terms were significantly enriched in the In7 subgroup, 10 in the In10 subgroup, 5 in the In14 subgroup and 4 in the In21 subgroup (Fig. 4A; Additional file 1: Table S5). The results of the KEGG pathway enrichment analysis were similar to those of the GO enrichment analysis, and the number of significantly enriched pathways decreased with age (Fig. 4B; Additional file 1: Table S6).

A total of 135 genes were found in the four groups by Venn diagram analysis (Fig. 4C; Additional file 1: Table S7). The 135 genes were clustered and partitioned by K-means, and the results were divided into 6 regions with different expression patterns (Additional file 1: Table S8). The FPKM values of the six regions were analysed, and the expression levels of genes in the red, yellow, blue and orange regions were significantly different between the challenge group and the control group (Fig. 4D). The expression trends of the 4 modular genes were determined.

Furthermore, we performed another Venn diagram analysis based on the genes enriched in the biological process (BP) GO category (GO0051607: defence response to virus; GO0006955: immune response) and the genes involved in the enriched KEGG pathways (apla04060: Cytokine—cytokine receptor Interaction; apla04622: RIG-1-like receptor signalling pathway; apla05164: Influenza A) and the expression trends of the 4 modular genes. Finally, 7 key genes were identified (Fig. 4E; Additional file 1: Table S9).

According to the LEfSe analysis, six key microbes were identified, including four that were consistently present before and after infection and two that showed discrepancies (Fig. 3C); additionally, Mantel test analysis was performed on these six microbes with the seven key candidate genes. *Candidatus Arthromitus* was significantly correlated with *DHX58*, *IFIH1* and LOC101798847 at 7 days of age. There was no significant correlation between DEGs and differentially abundant microbes in the 10- and 14-day-old groups. In the 21-day-old group, six differentially abundant microbes were significantly associated with the candidate DEGs, among which *DHX58* was significantly associated with five microbes, followed by *IFIH1* and *LOC101798847* (Fig. 4F; Additional file 1: Table S10). Interestingly, three genes, *DHX58*, *IFIH1* and *LOC101798847,* are involved in the same signalling pathway, namely, IFIH1-mediated induction of interferon-alpha/beta signalling.

3.6. Identification of key age-related microbes and genes related to resistance to DHAV-3 infection

In addition, the differentially abundant microbes of C7 v.s. C21 and In7 v.s. In21 groups were identified, and KEGG and COG functional enrichment were performed. The differentially abundant microbes in the C7 vs. C21 comparison were enriched in 155 pathways. Nineteen disease-related pathways were selected, and 3 immunity-related pathways, Fc gamma R-mediated phagocytosis, the RIG-1-like receptor signalling pathway and the haematopoietic cell lineage, were found to be significantly different between 7-day-old and 21-day-old ducklings (Fig. 5A; Additional file 1: Table S11). These pathways mainly perform two functions: information storage and processing and cellular processes and signalling.

Candidatus Arthromitus and *Bacteroides* were the dominant microbes in the C7 and C21 groups, respectively. The abundance of *Candidatus Arthromitus* decreased significantly in the 7-day-old group after DHAV-3 infection, but it was still the most abundant taxon. Similarly, the abundances of *Candidatus Arthromitus*, *Romboutsia*, *Corynebacterium* and *Enterococcus* increased significantly, and these became the main microbes in 21-day-old ducklings (Fig. 5B).

The expression levels of genes involved in IFIH1-mediated induction of the interferon-alpha/beta pathway were compared between In7 and In21 cells. The results showed that the abundances of these genes related to this pathway were significantly greater in the In7 group than in the

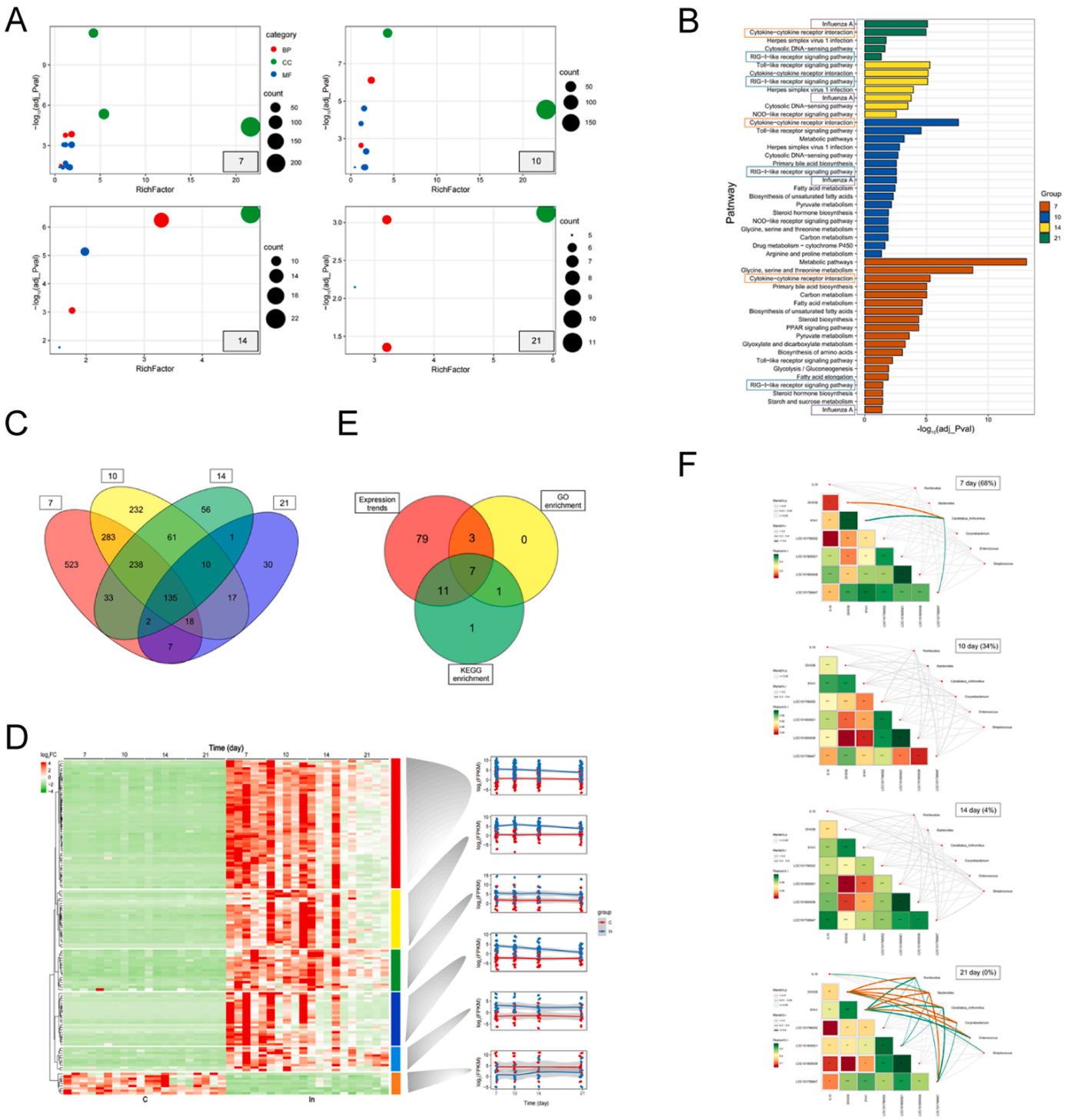

Fig. 4. Screening of candidate genes and Mantel correlation analysis of differentially abundant microbes. **A**. GO enrichment analysis of differentially expressed genes (DEGs) in the livers of ducklings at 7, 10, 14, and 21 days after infection. **B**. KEGG enrichment analysis of differentially expressed genes in the livers of 7-, 10-, 14-, and 21-day-old ducklings. Boxes indicate pathways that were significantly enriched in each group. **C**. Venn diagram analysis of DEGs in the livers of ducklings at 7, 10, 14, and 21 days after hatching. **D**. Heatmap analysis of the genes obtained from the venn diagram analysis was performed using the K-means method, and the expression trends of the DEGs according to age were shown. **E**. Venn diagram analysis of DEGs obtained from GO enrichment, KEGG enrichment, and venn diagram analyses. The variation in the level of expression with age for the DEGs was shown. **F**. Pairwise comparisons of differentially abundant microbes and candidate DEGs were shown. The level of expression of DEGs was related to each phenotype by partial (geographic distance–corrected) Mantel tests. The edge width indicates Mantel's r statistic for the corresponding distance correlations, and the edge colour indicates the statistical significance based on 9999 permutations. Boxes indicate the mortality rates for each group infected with DHAV-3.

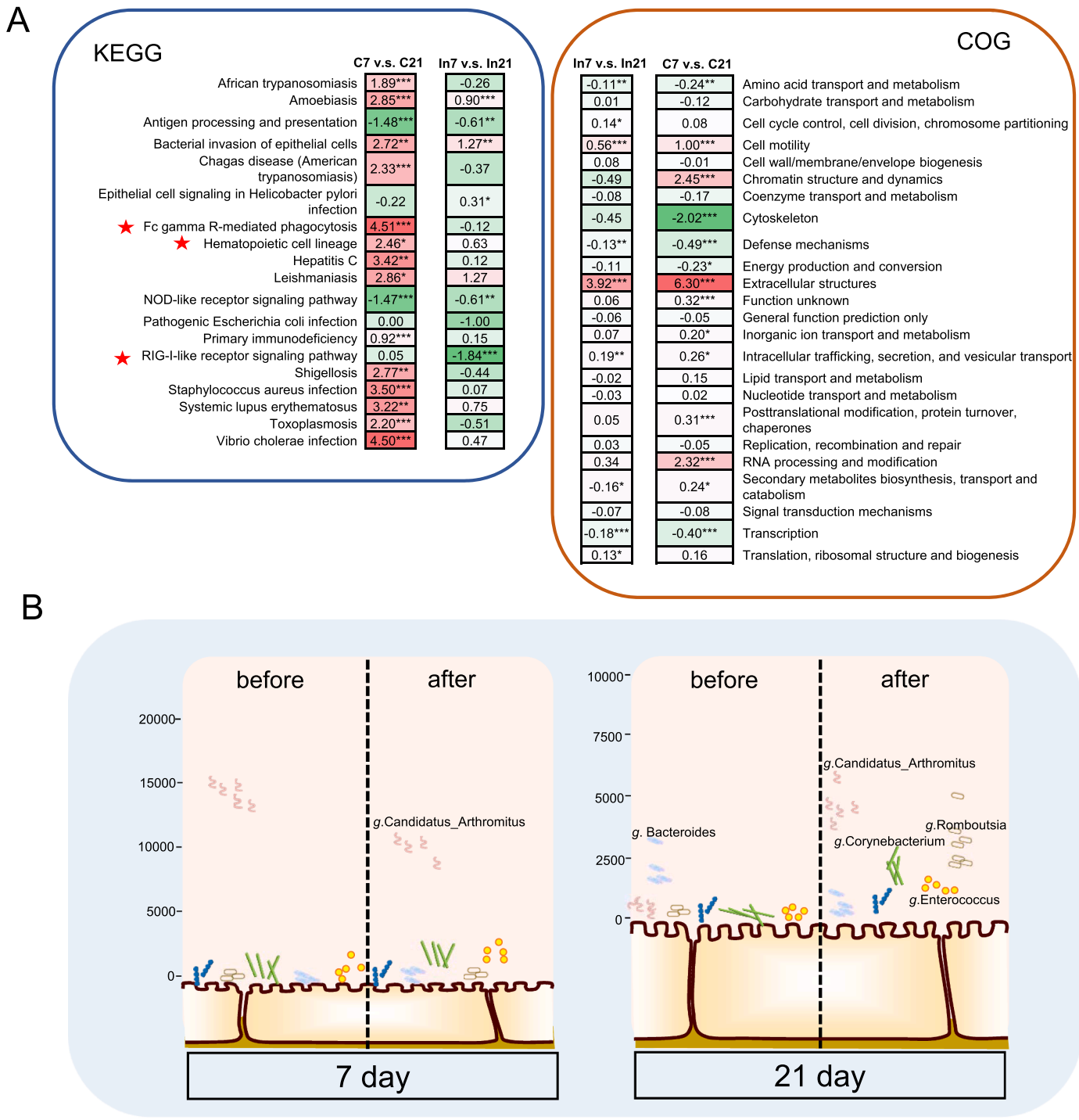

Fig. 5. Functional prediction analysis of microbes in the ileum at 7 and 21 days of age before and after infection with DHAV-3. **A**. The results were divided into two modules, KEGG (left) and COG (right). The number indicates the $\log_2$FoldChange. A positive value indicates that the pathway was upregulated at 7 days of age. **B**. Comparative analysis of differentially abundant microbes at 7 and 21 days of age. Variance analysis was performed using graphical presentation (below).

In21 group (Fig. 6A). The expression of these genes was significantly upregulated at 7 days after DHAV-3 infection (Fig. 6B-F). *IFIH1* is the key sensor that induces the IFN-I needed for CD8(+) T-cell responses; thus, the percentages of CD8(+) T cells in both groups were also examined, with higher numbers of CD8(+) T cells being found in the In7 group ($P < 0.05$; Fig. 7). The results suggested that 7-day-old ducklings produced more interferon and CD8(+) T cells after infection with DHAV-3.

4. Discussion

As Pekin ducks are an important part of the meat industry, they are suitable for the selection and breeding of mating lines for meat duck [33]. In this study, the microbial compositions of the ileum and caecum at different ages (days after hatching) were compared. We found that the ileal microbial composition and changes in microbial composition varied with age. We analysed the ileal microbiota of ducks of different ages before and after DHAV-3 infection, and six microbes at the genus level were significantly different between the 7-day-old and 21-day-old

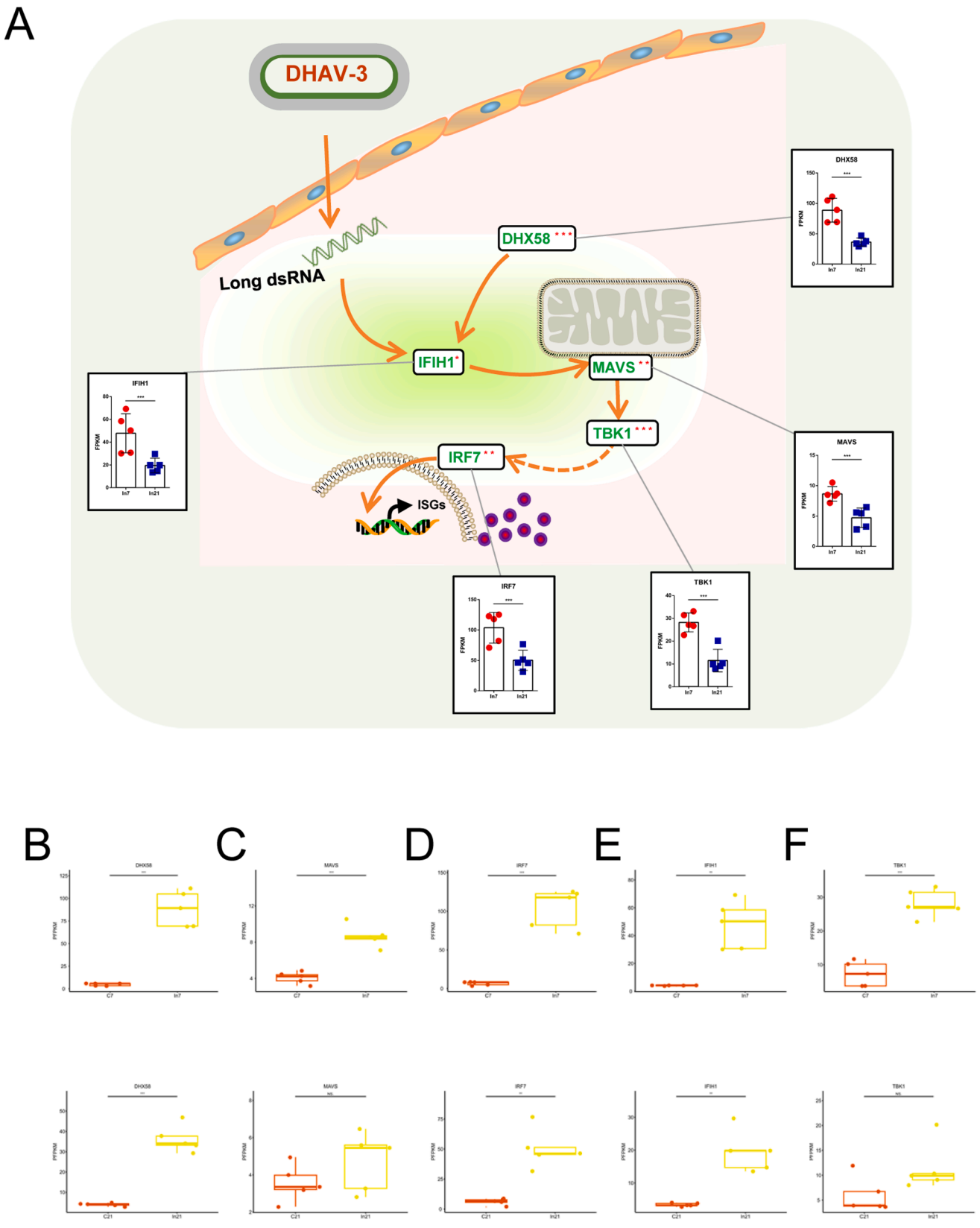

Fig. 6. Demonstration and analysis of the involvement of differentially expressed genes in pathways. **A**. Differences in the expression of genes involved in IFIH1-mediated induction of the interferon-alpha/beta pathway in the liver were compared between the 7- and 21-day-old groups after infection with DHAV-3. * , $P < 0.05$; ** , $0.05 < P < 0.01$; *** , $P < 0.001$. Expression levels of *DHX58* (**B**), *MAVS* (**C**), *IRF7* (**D**), *IFIH1* (**E**) and *TBK1* (**F**) in the livers of 7-day-old and 21-day-old Pekin ducks before and after infection with DHAV-3. NS, $P > 0.05$; ** , $0.05 < P < 0.01$; *** , $P < 0.001$.

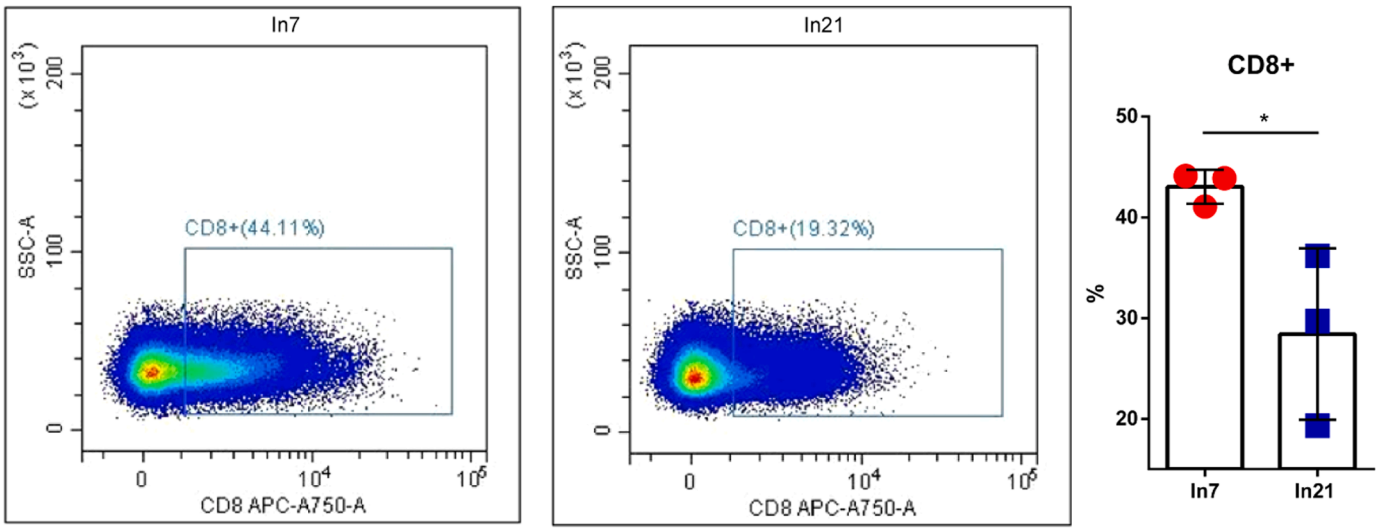

Fig. 7. The levels of CD8(+) T cells in the blood at 7 and 21 days of age were compared after infection with DHAV-3 * , $P < 0.05$.

ducklings. Additionally, seven genes associated with DHAV-3 infection were identified by RNA-seq, and these genes were significantly associated with microbes in the 7-day-old and 21-day-old groups. These seven candidate genes are involoved in IFIH1-mediated induction of the interferon α/β pathway, stimulating the production of interferons and CD8(+) T cells.

Phenotypic data revealed that IgA and CRP levels significantly increased in the blood of C21 ducks and that the CRP concentration decreased after DHAV3 infection in 21-day-old ducks. We believe that the presence of IgA and CRP at a certain level allows for rapid activation of a highly effective anti-infective immune response at any time; therefore, at 21 days of age, there is strong DHAV-3 resistance in the same feeding environment. To determine the effect of age on intestinal microbes, the host genetic background, feeding environment, and feed composition were controlled. The function of the duck intestine is closely related to the spatial distribution of the ileal and caecal flora. Therefore, using microbes from the ileum and caecum of these ducks at different ages, we showed that the composition of ileal microbes was more susceptible to the effects of age (Fig. 1E), which was consistent with the findings related to the effect of age on the intestinal flora of broiler chickens [34]. This laid the foundation for our subsequent experiments.

Viral infection strongly alters the structure of the intestinal microbiota [35]. We analysed the microflora in the ileum of Pekin ducks of the same age group before and after DHAV-3 infection. *Candidatus Arthromitus* was found to be the dominant genus in 7-day-old ducks and remained the dominant genus after infection with DHAV-3, although its abundance decreased significantly. *Candidatus Arthromitus* is an important microbe that drives the development of T helper 17 (Th17) cells in the gastrointestinal tract [36]. It can directly reduce the enterovirus load and affect the migration and shedding of enterocytes by promoting epithelial cell proliferation/replacement-related gene expression, which in turn affects viral passage rates and alters host viral resistance [37]. This difference might also explain the significant increase in the abundance of *Candidatus Arthromitus* in the ileum of 21-day-old ducklings infected with DHAV-3 (Fig. 5B). Viral infection also increased the abundance of some microbes that are harmful to the host, e.g., *Romboutsia*, *Corynebacterium*, and *Enterococcus*, in 21-day-old ducklings. In this study, the percentage of beneficial bacteria decreased significantly, and the percentage of other microbial genera increased from 6.8% to 40.9% in 7-day-old ducklings. However, in 21-day-old ducklings, the increase in the level of beneficial bacteria was extremely significant, and the abundance of other microbial genera decreased from 82.7% to 32.1%, which significantly changed the microbial structure of both groups. This difference might be related to the differences in resistance to DHAV-3 in both age groups (Fig. 5B). Moreover, the findings of these studies suggested that some probiotics, such as *Candidatus Arthromitus*, could be appropriately added to the diet to improve the resistance of ducks to DHAV-3.

The intestinal flora communicates with the liver via the portal vein and bile ducts. The liver is the largest immune organ and target organ for DHAV-3 infection. Hence, we collected liver tissues for transcriptome sequencing and identified seven key DEGs. Analysis of the correlations between DEGs and differentially abundant microbes showed correlations only in the 7-day-old and 21-day-old ducklings, probably due to extreme phenotypic differences. The differences in the microbial communities between 7-day-old and 21-day-old ducklings were compared based on the KEGG pathway analysis, and the $\log_2$FoldChange of the immune system pathways between C7 and C21 was 1.5-fold greater than that between In7 and In21 ($P < 0.05$; Fig. 5A). We found significant differences in antigen recognition (haematopoietic cell lineage and the RIG-I-like receptor signalling pathway) and clearance (Fc gamma R-mediated phagocytosis) between 7-day-old and 21-day-old ducklings. Haematopoietic stem cells can differentiate into a common lymphoid progenitor or a common myeloid progenitor [38], and specific retinoic acid-inducible gene 1-like receptors (including *RIG-1*, *MDA5*, and *LGP2*) are responsible for detecting viral pathogens [39]. The above two pathways are essential for the development of the innate immune response. Additionally, Fc gamma receptors recognize pathogens and strongly influence host defence by taking up and destroying infectious pathogens [40]. This might partly explain the greater susceptibility of younger ducklings.

The MDA5 protein, encoded by the gene *IFIH1*, is a key participant in the RIG-1 signalling pathway, suggesting a link between the intestinal and liver tissue. IFIH1 is the key sensor that induces IFN-I needed for CD8(+) T-cell responses, and Fc gamma receptors can mediate the activation of T cells [41]. To determine whether this pathway differed between 7-day-old and 21-day-old ducklings, the percentages of CD8(+) T cells in both groups were examined. CD8(+) T cells are responsible for destroying infected cells. The presence of many CD8(+) T cells indicates that many cells are infected, as observed in this study. The long double-stranded RNA (dsRNA) produced during replication by picornaviruses can be detected in MDA5 [42], and DHAV-3 is a member of the family *Picarnoviridae* (https://www.picornaviridae.com22vihepatovirus22vihepatoviruss.html). However, whether the dsRNA produced during DHAV-3 replication interacts directly with *MDA5* requires further investigation. This result also provides a basis for further investigation into the pathogenesis of DHAV-3 to identify more effective

molecular tags for disease resistance breeding.

In this study, we investigated the changes in intestinal microbes within the same genetic background and their relationship with disease resistance from the perspectives of age-related changes and viral infection. We found that intestinal microbes participate in age-related changes and disease resistance, which provides new information for understanding the susceptibility of young animals to viruses and lays the foundation for subsequent breeding programs for enhancing disease resistance.

Furthermore, the microbial composition in the ileum was correlated with age (in days). Six microbes exhibited significant differences in abundance after infection with DHAV-3. These microbes were significantly associated with seven immune-related DEGs in 7-day-old and 21-day-old ducklings. Among the seven DEGs, *IFIH1* and *DHX58* were involved in the pathways that induce interferon and CD8(+) T-cell production. Our findings provide a comprehensive understanding of the susceptibility of ducklings of different ages to viruses.

Ethics approval and consent to participate

Not applicable.

Ethics

Animal experiments were performed following the guidance and under the approval of the Animal Welfare and Ethics Committee of China Agricultural University and the animal care and use committee of the Institute of Animal Sciences of the Chinese Academy of Agricultural Sciences (IAS2022–116).

Consent for publication

Not applicable.

CRediT authorship contribution statement

Suyun Liang: Methodology, Data curation, Investigation, Writing – original draft. **Shuisheng Hou:** Resources, Data curation, Supervision, Funding acquisition. **Meixi Lu**: Data curation, Validation, Writing – review & editing. **Daxin Yu**: Data curation, Methodology. **Guangnan Xing**: Data curation, Methodology. **Zhanqing Ji:** Data curation, Methodology, **Zhanbao Guo**: Investigation. **Qi Zhang**: Investigation. **Wei Huang:** Investigation. **Ming Xie**: Investigation. All authors read and approved the final manuscript.

Declaration of Competing Interest

The authors declare that they have no competing interests.

Data Availability

The raw sequence data reported in this paper have been deposited in the Genome Sequence Archive (Genomics, Proteomics & Bioinformatics 2021) in the National Genomics Data Center (Nucleic Acids Res 2022), China National Center for Bioinformation/Beijing Institute of Genomics, Chinese Academy of Sciences and are publicly accessible at https://ngdc.cncb.ac.cn/gsa. The accession number of the 16 S dataset is CRA010045, and the accession number of the transcriptome dataset is CRA010098.

Acknowledgements

This study was supported by the Chinese Agricultural and Research System of the Ministry of Agriculture (CARS-42).

Appendix A. Supporting information

Supplementary data associated with this article can be found in the online version at doi:10.1016/j.csbj.2024.01.005.

References

[1] de Mesquita Souza Saraiva M, Lim K, do Monte DFM, Givisiez PEN, Alves LBR, de Freitas Neto OC, Kariuki S, et al. Antimicrobial resistance in the globalized food chain: a one health perspective applied to the poultry industry. Braz J Microbiol 2022:465–86.
[2] Bryant RB, Endale DM, Spiegal SA, Flynn KC, Meinen RJ, Cavigelli MA, et al. Poultry manureshed management: opportunities and challenges for a vertically integrated industry. J Environ Qual 2022;51:540–51.
[3] Liang S, Zhang J, Wang X, Xing G, Guo Z, Zhang Q, et al. Selective analysis of resistance and susceptibility to duck hepatitis A virus genotype 3 in Pekin duck. Animal Res. One Health 2023;2:146–55.
[4] Patil SS, Shinduja R, Suresh KP, Phukan S, Kumar S, Sengupta PP, et al. A systematic review and meta-analysis on the prevalence of infectious diseases of Duck: a world perspective. Saudi J Biol Sci 2021;28:5131–44.
[5] Makagon MM, Riber AB. Setting research driven duck-welfare standards: a systematic review of Pekin duck welfare research. Poult Sci 2022;101:101614.
[6] Best AA, Porter AL, Fraley SM, Fraley GS. Characterization of gut microbiome dynamics in developing pekin ducks and impact of management system. Front Microbiol 2017:2125.
[7] Zhu C, Song W, Tao Z, Liu H, Zhang S, Xu W, et al. Analysis of microbial diversity and composition in small intestine during different development times in ducks. Poult Sci 2020;99:1096–106.
[8] Ma N, Tian Y, Wu Y, Ma X. Contributions of the interaction between dietary protein and gut microbiota to intestinal health. Curr Protein Pept Sci 2017;18:795–808.
[9] Wang G, Huang S, Wang Y, Cai S, Yu H, Liu H, et al. Bridging intestinal immunity and gut microbiota by metabolites. Cell Mol Life Sci 2019;76:3917–37.
[10] Wang X, Sun G, Feng T, Zhang J, Huang X, Wang T, et al. Sodium oligomannate therapeutically remodels gut microbiota and suppresses gut bacterial amino acids-shaped neuroinflammation to inhibit Alzheimer's disease progression. Cell Res 2019;29:787–803.
[11] Schuijt TJ, Lankelma JM, Scicluna BP, de Sousa e Melo F, Roelofs JJ, de Boer JD, et al. The gut microbiota plays a protective role in the host defence against pneumococcal pneumonia. Gut 2016;65:575–83.
[12] Cyr B, de Rivero Vaccari JP. Age-dependent microglial response to systemic infection. Cells 2021;10:1037.
[13] Goldstein E, Nguyen HH, Liu P, Viboud C, Steiner CA, Worby CJ, et al. On the relative role of different age groups during epidemics associated with respiratory syncytial virus. J Infect Dis 2018;217:238–44.
[14] Bruns EB, Hood ME, Antonovics J, Ballister IH, Troy SE, Cho JH. Can disease resistance evolve independently at different ages? Genetic variation in age-dependent resistance to disease in three wild plant species. J Ecol 2022;110:2046–61.
[15] Anderson RM, Grenfell BT, May RM. Oscillatory fluctuations in the incidence of infectious disease and the impact of vaccination: time series analysis. J Hyg (Lond) 1984;93:587–608.
[16] Colditz IG, Watson DL, Gray GD, Eady SJ. Some relationships between age, immune responsiveness and resistance to parasites in ruminants. Int J Parasitol 1996;26:869–77.
[17] Yugo DM, Hauck R, Shivaprasad HL, Meng XJ. Hepatitis virus infections in poultry. Avian Dis 2016;60:576–88.
[18] OIE. OIE Terrestrial Manual 2019. 2019. Duck Virus Hepatitis.
[19] Doan HT, Le XT, Do RT, Hoang CT, Nguyen KT, Le TH. Molecular genotyping of duck hepatitis A viruses (DHAV) in Vietnam. J Infect Dev Ctries 2016;10:988–95.
[20] Wen X, Zhu D, Cheng A, Wang M, Chen S, Jia R, et al. Molecular epidemiology of duck hepatitis a virus types 1 and 3 in China, 2010-2015. Transbound Emerg Dis 2018;65:10–5.
[21] Wang X, Zhang J, Meng R, Jiang Y, Liang S, Zhang Y, et al. Host differences affecting resistance and susceptibility of the second generation of a pekin duck flock to duck hepatitis A virus genotype 3. Front Microbiol 2017;8:1128.
[22] Zheng LS. Detection of Pathogens Associated with Duck Viral Hepatitis and Preparation of A Virulent Duck Hepatitis A Virus 3. Beijing: China Agricultural University; 2014. 43 p.
[23] Ministry of Agriculture of China. Nutrient Requirements of Meat-Type Ducks of China. Beijing, China: China Agriculture Press; 2012.
[24] Kechin A, Boyarskikh U, Kel A, Filipenko M. cutPrimers: a new tool for accurate cutting of primers from reads of targeted next generation sequencing. J Comput Biol: A J Comput Mol Cell Biol 2017;24:1138–43.
[25] Callahan BJ, McMurdie PJ, Rosen MJ, Han AW, Johnson AJ, Holmes SP. DADA2: high-resolution sample inference from Illumina amplicon data. Nat Methods 2016;13:581–3.
[26] Hall M, Beiko RG. 16S rRNA gene analysis with QIIME2. Methods Mol Biol 2018;1849:113–29.
[27] Wingett SW, Andrews S. FastQ screen: a tool for multi-genome mapping and quality control. F1000Res 2018;24:1338.
[28] Dobin A, Gingeras TR. Mapping RNA-seq reads with STAR. Curr Protoc Bioinforma 2015;51. pp. 11.14.1-11.14.19.
[29] Li B, Dewey CN. RSEM: accurate transcript quantification from RNA-Seq data with or without a reference genome. BMC Bioinforma 2011;12:323.

[30] Love MI, Huber W, Anders S. Moderated estimation of fold change and dispersion for RNA-seq data with DESeq2. Genome Biol 2014;15:550.
[31] Liang S, Hu X, Guo Z, Luo D, Tang J, Ji Z, et al. Comparative transcriptome reveals the effect of IFITM1 on differential resistance to duck hepatitis A virus genotype 3 in Pekin ducks. Virus Res 2022;322:198930.
[32] H.Y. Huang. linkET: Everything is Linkable. R package version 0.0.3.2021.
[33] Zheng A, Liu G, Zhang Y, Hou S, Chang W, Zhang S, et al. Proteomic analysis of liver development of lean Pekin duck (Anas platyrhynchos domestica). J Proteom 2012;75:5396–413.
[34] Shibata M, Takahashi T, Endo K, Kozakai T, Azuma Y, Kurose Y. Age-related regulation of active amino acid transport in the ileum of broiler chickens. J Poult Sci 2020;57:131–7.
[35] Kim AH, Hogarty MP, Harris VC, Baldridge MT. The complex interactions between rotavirus and the gut microbiota. Front Cell Infect Microbiol 2021;10:586751.
[36] Kumar P, Monin L, Castillo P, Elsegeiny W, Horne W, Eddens T, et al. Intestinal interleukin-17 receptor signaling mediates reciprocal control of the gut microbiota and autoimmune inflammation. Immunity 2016;44:659–71.
[37] Shi Z, Zou J, Zhang Z, Zhao X, Noriega J, Zhang B, et al. Segmented filamentous bacteria prevent and cure rotavirus infection. Cell 2019;179. pp. 644-658.e13.
[38] Akashi K, Traver D, Miyamoto T, Weissman IL. A clonogenic common myeloid progenitor that gives rise to all myeloid lineages. Nature 2000;404:193–7.
[39] Loo YM, Gale M. Immune signaling by RIG-I-like receptors. Immunity 2011;34:680–92.
[40] Junker F, Gordon J, Qureshi O. Fc gamma receptors and their role in antigen uptake, presentation, and T cell activation. Front Immunol 2020;11:1393.
[41] Wang Y, Swiecki M, Cella M, Alber G, Schreiber RD, Gilfillan S, et al. Timing and magnitude of type I interferon responses by distinct sensors impact CD8 T cell exhaustion and chronic viral infection. Cell Host Microbe 2012;11:631–42.
[42] Feng Q, Hato SV, Langereis MA, Zoll J, Virgen-Slane R, Peisley A, et al. MDA5 detects the double-stranded RNA replicative form in picornavirus-infected cells. Cell Rep 2012;2:1187–96.